Wave-function-renormalization effects in resonantly enhanced tunneling

N. Lörch,[1] F. V. Pepe,[2,3] H. Lignier,[4] D. Ciampini,[5,6] R. Mannella,[5] O. Morsch,[6] E. Arimondo,[5,6] P. Facchi,[3,7] G. Florio,[2,3,*] S. Pascazio,[2,3] and S. Wimberger[1,8]

[1]*Institut für Theoretische Physik, Universität Heidelberg, Philosophenweg 19, D-69120 Heidelberg, Germany*
[2]*Dipartimento di Fisica and MECENAS, Università di Bari, I-70126 Bari, Italy*
[3]*INFN, Sezione di Bari, I-70126 Bari, Italy*
[4]*Laboratoire Aimé Cotton, Université Paris-Sud, Batiment 505, Campus d'Orsay, F-91405 Orsay Cedex, France*
[5]*CNISM-Pisa, Dipartimento di Fisica, Università di Pisa, Lgo Pontecorvo 3, I-56127 Pisa, Italy*
[6]*INO-CNR, Dipartimento di Fisica, Università di Pisa, Lgo Pontecorvo 3, I-56127 Pisa, Italy*
[7]*Dipartimento di Matematica and MECENAS, Università di Bari, I-70125 Bari, Italy*
[8]*Center for Quantum Dynamics, Universität Heidelberg, D-69120 Heidelberg, Germany*

(Received 30 January 2012; published 3 May 2012)

We study the time evolution of ultracold atoms in an accelerated optical lattice. For a Bose-Einstein condensate with a narrow quasimomentum distribution in a shallow optical lattice the decay of the survival probability in the ground band has a steplike structure. In this regime we establish a connection between the wave-function-renormalization parameter Z introduced by P. Facchi, H. Nakazato, and S. Pascazio [Phys. Rev. Lett. **86**, 2699 (2001)] to characterize nonexponential decay and the phenomenon of resonantly enhanced tunneling, where the decay rate is peaked for particular values of the lattice depth and the accelerating force.

DOI: 10.1103/PhysRevA.85.053602 PACS number(s): 03.75.Lm, 03.65.Xp

I. INTRODUCTION

Resonantly enhanced tunneling (RET) is a quantum effect in which the probability for the tunneling of a particle between two potential wells is increased when the quantized energies of the initial and final states of the process coincide. In spite of the fundamental nature of this effect [1] and its practical interest [2], it has been difficult to observe it experimentally in solid-state structures. Since the 1970s, much progress has been made in constructing solid-state systems such as superlattices [3–5] and quantum wells [6], which enable the controlled observation of RET [7].

In recent years, ultracold atoms in optical lattices [8,9], arising from the interference pattern of two or more intersecting laser beams, have been increasingly used to simulate solid-state systems [9–11]. Optical lattices are easy to realize in the laboratory, and the parameters of the resulting one-, two-, or three-dimensional periodic potentials (the lattice spacing and the potential depth) can be perfectly controlled both statically and dynamically. In Refs. [12,13], a Bose-Einstein condensate (BEC) in accelerated optical lattice potentials was used to study the phenomenon of RET. In a tilted periodic potential, atoms can escape by tunneling to the continuum via higher-lying levels. Within the RET process the tunneling of atoms out of a tilted lattice is resonantly enhanced when the energy difference between lattice wells matches the distance between the energy levels in the wells.

The atomic temporal evolution is described by the survival probability, starting from an initial state prepared in the ground band of the lattice. At long interaction times, after several tunneling processes, the survival probability is characterized by an exponential decay rate with a constant tunneling probability for each Bloch period [14]. Such a decay was examined in different theoretical analyses [5,6,14] and measured in experimental investigations with ultracold atoms [12,13,15,16]. In this study we scrutinize the time behavior of the tunneling probability and use its remarkable features at short and intermediate times in order to extract information about wave-function-renormalization effects.

The key quantity in this context is the probability that the system investigated "survives" in a given state (or a set of states, such as a band of a lattice). In this article we shall deal with survival probabilities whose behavior is complex and difficult to analyze. See, for example, the experimental results of Ref. [15] and Figs. 2 and 5 below, which display the survival probability of a cloud of ultracold atoms in the ground band of an accelerated optical lattice. Clearly, one can properly speak of the "decay" associated with an unstable system (the atoms tend to leak out of the accelerated lattice), but the time evolution can display oscillations or even plateaus. (As we shall see, the latter are easily understood in terms of the initial atomic state.)

General theoretical considerations show that the (adiabatic) survival probability of an unstable system can often be written as

$$P(t) = Z \exp(-\gamma t) + \text{additional contributions}, \qquad (1)$$

where γ is the decay rate, which can be computed by the Fermi golden rule. The parameter Z, representing the extrapolation of the asymptotic decay law back to $t = 0$, is related to wave-function renormalization, and the additional contribution is due to the background integral in the energy plane. Law (1) is valid both in quantum mechanics [17,18] and quantum field theory [19,20], and Z can be smaller or larger than unity [21].

Typically, the additional contributions in Eq. (1) dominate both at short and long times, where the exponential decay law is superseded by a quadratic [22–24] and a power law [25], respectively. They are therefore crucial in order to cancel the exponential in these time domains. However, they can play a

[*]Present address: Museo Storico della Fisica e Centro Studi e Ricerche "Enrico Fermi", Piazza del Viminale 1, 00184 Rome, Italy.

key role in a much more general context, such as the RET phenomenon to be investigated in this article.

The pioneering experiments performed in Texas, with Landau-Zener transitions in cold atoms, checked the existence of the short-time quadratic behavior [26] and the transition [27] from the quantum Zeno effect [23] to the anti- or inverse-Zeno effect [28–30], through a sequence of properly tailored quantum measurements.

With the arrival of Bose-Einstein condensates the experimental resolution has advanced even further compared to cold atoms. While cold atoms can have a momentum distribution on the order of a Brillouin zone or more, a very narrow distribution (much smaller than a Brillouin zone) is achievable with BECs. Even the steplike structure of the survival probability occurring for shallow lattice depth can be resolved with great precision [15,16]. It is in this regime of shallow lattices and short jump times [31] where the yet unobserved link of RET and the initial deviation from exponential decay is most striking. This work is devoted to the study of these effects. The choice of a different initial atomic state, with a well-defined momentum, will enable us to observe a more complicated temporal structure. We shall therefore scrutinize the time evolution in order to unveil an exponential regime and introduce the Z parameter in our RET framework.

This paper is organized as follows. We briefly sum up previous results on RET in Sec. II. We then analyze the dynamics in the tilted lattice in Sec. III, and we show in Sec. IV, the main part of this article, how the two phenomena arise as interference effects. Section V reports experimental results for the wave-function-renormalization parameter Z in the case of a Bose-Einstein condensate in an accelerated optical lattice and also a comparison with the experimental configuration by Wilkinson *et al.* [26]. Section VI concludes our work.

II. LANDAU-ZENER AND RESONANTLY ENHANCED TUNNELING

A Landau-Zener (LZ) transition takes place in a system with a time-dependent Hamiltonian, in which the spectrum, as a function of a control parameter (here time t), is characterized by the presence of an avoided crossing [32–36]. A LZ transition is described by the following two-level Hamiltonian:

$$H_{\mathrm{LZ}}(t) = \begin{pmatrix} \alpha t & \delta E/2 \\ \delta E/2 & -\alpha t \end{pmatrix}, \tag{2}$$

written in a suitable basis, known as the *diabatic basis*. The energy separation of the diabatic states varies linearly with time, i.e., as $2\alpha t$ from Eq. (2). The coupling $\delta E/2$ between the states is constant and induces an avoided level crossing. The diagonalization of Eq. (2) yields the instantaneous eigenvalues,

$$E_{\pm} = \pm\sqrt{(\alpha t)^2 + \left(\frac{\delta E}{2}\right)^2}. \tag{3}$$

The eigenbasis of $H_{\mathrm{LZ}}(t)$ is called the *adiabatic basis*. At $t \to -\infty$ the adiabatic energy levels of Eq. (3) are infinitely separated, and no transition between them occurs. The distance between the levels decreases toward the avoided crossing at $t = 0$ and then increases again until, at $t \to \infty$, the separation becomes again infinite. If the system is prepared at $t \to -\infty$ in one of the adiabatic eigenstates, the probability that the system undergoes a transition at $t \to \infty$ toward the other adiabatic eigenstate reads [33]

$$P_{\mathrm{LZ}} = \exp\left(-\frac{\pi(\delta E)^2}{4\hbar\alpha}\right). \tag{4}$$

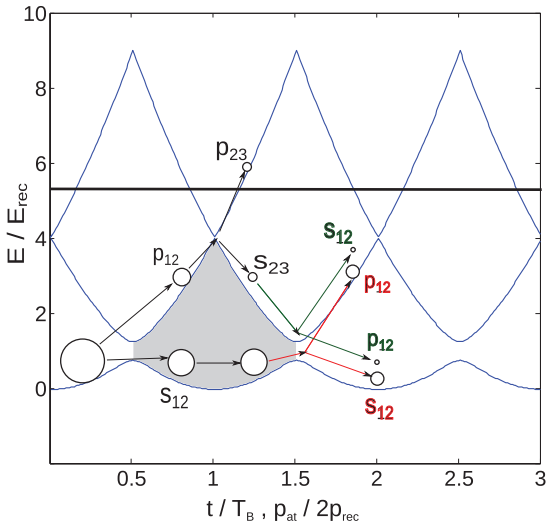

FIG. 1. (Color online) Energy diagram for a particle in a periodic potential vs either the time, in units of Bloch time T_{B} defined in Eq. (14), or the atomic momentum, $p_{\mathrm{at}}/2p_{\mathrm{rec}}$, where $p_{\mathrm{rec}} = \hbar\pi/d_L$ units. Under the application of an external force, the quasimomentum increases with time, and at the avoided crossing between two bands, at the edge of the Brillouin zone, where $p_{\mathrm{at}} = p_{\mathrm{rec}}$, the condensate tunnels with a probability amplitude p_{ij} and survives with an amplitude s_{ij}, defined in Eq. (22). Between two avoided crossings of the lowest two bands a relative phase ϕ, defined in Eq. (17), is acquired, which is graphically displayed as a shaded area. The final survival probability at a given time is the sum over all possible routes, just like a path integral in momentum space.

A particle in a shallow periodic potential, subjected to an external force, is an example of a physical system in which a LZ process can be observed. In this case, the diabatic basis is represented by the momentum eigenstates. As schematized in Fig. 1, if the system is initially prepared in the lowest band, with a very peaked momentum distribution around $p = 0$, it will evolve toward the edge of the first Brillouin zone, where the distance between the first and the second bands is minimal and transitions are more likely to occur, and then it evolves back to the bottom of the first band. The transition probability toward the second band in this process can be approximated by P_{LZ}, but discrepancies can arise due to the differences between the idealized case, leading to the LZ formula (4), and the real physical situation. Indeed, the periodicity of the lattice implies that the aforementioned process occurs in a *finite* time and that in the initial and final states the adiabatic levels are not infinitely separated. The corrections to the LZ transition probability due to the finite duration of the process are discussed in Refs. [16,37].

Other corrections to Eq. (4) should be considered if the lattice is not shallow. In this case, couplings to higher-momentum states play an important role, and a two-level description is no longer a good approximation.

Moreover, there is another kind of deviation from LZ, which will be the main object of our analysis. Since Eq. (4) is obtained under the hypothesis that only one of the two adiabatic eigenstates is initially populated, it is no longer valid if both states are populated. These deviations can be relevant even if one of the initial populations is very close to zero since their order is the *square root* of the smaller population, as will be discussed in the following. In a periodic potential, tilted by an external force F, the probability that a wave packet initially prepared in the first band jumps to the second band corresponds to the LZ prediction (4) only if the second band is empty. A small population in the second band gives rise to oscillations around P_{LZ}.

Finally, the transition probability is enhanced by a large factor with respect to the LZ prediction if the energy difference $Fd_L\Delta i$ between two potential wells (d_L being the lattice spacing and $d_L\Delta i$ being the distance between the wells) matches the average band gap of the nontilted system (RET). One expects that in a RET process, from the first band to the second band, the asymptotic regime will only be reached after a transient period. Indeed, while the first transition occurs when the second band is strictly empty (and thus the tunneling event closely follows the LZ prediction), further RET transitions will occur periodically in time and, starting from the second tunneling process, interference effects due to the finite population amplitude in the second band will start to play an important role, modifying the time evolution in an important way.

The analysis of the following two sections will endeavor to take all these effects into account. We shall build up an effective model whose validity will be tested for rather diverse ranges of the parameters and compared to experimental results finally in Sec. V.

III. DYNAMICS OF INTERBAND TUNNELING

In our analysis we are interested in describing the RET process from the first band to the second band of a Bose-Einstein condensate loaded into an optical lattice. It will be assumed that almost all the particles of the system are in the condensate, so that the system is described by a single-particle wave function $\psi(x,t)$ [38]. Moreover, we will consider the condensate dilute enough so that the interaction between particles can be neglected. This implies that the wave function of the system obeys a linear Schrödinger equation. In order to operate away from the interaction-dominated regime explored, e.g., in Ref. [39], in the present experiment the condensate expands [15,16] and its density is reduced before the optical lattice is applied. Nonlinear effects, on the other hand, have been studied in the RET regime in other works [12,13,40–45].

The experimental condition is that of an accelerating one-dimensional optical lattice, with constant acceleration a. In the rest frame of the lattice, a particle of mass m sitting in the lattice is subjected to an external force $F = ma$, and thus the time-independent Hamiltonian of the system in this frame of reference reads

$$H = -\frac{\hbar^2}{2m}\frac{\partial^2}{\partial x^2} + \frac{V}{2}\cos\left(\frac{2\pi x}{d_L}\right) - Fx \equiv H_0 - Fx, \quad (5)$$

where V is the lattice depth and the lattice period d_L is half the wavelength of the counterpropagating lasers. H_0 represents the "unperturbed" Hamiltonian, whose eigenstates are the Bloch functions

$$\phi_{\alpha,k}(x) = e^{ikx}\chi_{\alpha,k}(x), \quad (6)$$

$$\chi_{\alpha,k}(x + d_L) = \chi_{\alpha,k}(x), \quad (7)$$

$$H_0\phi_{\alpha,k}(x) = \epsilon_\alpha(k)\phi_{\alpha,k}(x), \quad (8)$$

with $\alpha = 1,2,3,\ldots$ being the band index and k being the quasimomentum, ranging in the first Brillouin zone $\mathcal{B} = \{k| -\pi/d_L \leqslant k \leqslant \pi/d_L\}$. The dynamics of the system depends on two dimensionless parameters [16] related to lattice depth and external force:

$$V_0 = \frac{V}{E_{\mathrm{rec}}}, \quad F_0 = \frac{Fd_L}{E_{\mathrm{rec}}}, \quad \text{with} \quad E_{\mathrm{rec}} = \frac{\hbar^2}{2m}\left(\frac{\pi}{d_L}\right)^2, \quad (9)$$

where m is the mass of the atoms. Applying the unitary transformation

$$\tilde{\psi}(x,t) = \exp(-iFxt/\hbar)\psi(x,t) \quad (10)$$

restores the (discrete) translational invariance of the Hamiltonian at the expense of an explicit time dependence:

$$\tilde{H}(t) = \frac{1}{2m}\left(-i\hbar\frac{\partial}{\partial x} + Ft\right)^2 + \frac{V}{2}\cos\left(\frac{2\pi x}{d_L}\right). \quad (11)$$

Rewriting this Hamiltonian in the momentum basis as in Ref. [16] establishes the relation to the Landau-Zener Hamiltonian introduced in Eq. (2): To calculate the time evolution of any momentum eigenstate, we only need the Hamiltonian H_{k_0} acting on the subspace with a given quasimomentum k_0, as there is no transition between states with different k_0:

$$H_{k_0} = \frac{1}{2m}\begin{pmatrix} \ddots & & & & 0 \\ & \hbar^2\left(k - \frac{2\pi}{d_L}\right)^2 & mV/2 & & \\ & mV/2 & (\hbar k)^2 & mV/2 & \\ & & mV/2 & \hbar^2\left(k + \frac{2\pi}{d_L}\right)^2 & \\ 0 & & & & \ddots \end{pmatrix}, \quad (12)$$

where $k = k(t) = k_0 + Ft/\hbar$. This Hamiltonian (12) leads to a very accurate numerical solution of the Schrödinger equation. For small V on the scale of E_{rec} its dynamics is well described by successive Landau-Zener transitions, occurring whenever two diagonal terms in H_{k_0} become degenerate. We will use this approximation to obtain analytical results. In Fig. 1 the relevant transitions are depicted graphically.

We first examine an adiabatic approximation of the dynamics generated by the Hamiltonian (5), yielding no transition between bands (*single-band approximation*), which will highlight the time periodicity of the system and the phase differences between bands. We shall then introduce an effective coupling between the low-lying bands that enables one to obtain transition rates. The adiabatic approximation is consistent if $Fd_L \lesssim V$, namely, if $F_0 \lesssim V_0$ in Eq. (9).

The initial state will be assumed to be highly peaked around a single quasimomentum value k_0; that is, the width of the initial quasimomentum distribution will be taken to be much smaller than the width $2\pi/d_L$ of the first Brillouin zone $\mathcal{B}$. In this situation, it can be proved [36,37] that in the adiabatic single-band approximation the average quasimomentum evolves semiclassically, so that at time t,

$$k(t) = k_0 + \frac{Ft}{\hbar}, \tag{13}$$

with negligible spread in the quasimomentum distribution occurring during the evolution. This yields Bloch oscillations in a tilted lattice with a Bloch period

$$T_{\mathrm{B}} = \frac{2\pi\hbar}{Fd_L} = \frac{\hbar}{E_{\mathrm{rec}}}\frac{2\pi}{F_0}. \tag{14}$$

The initial state analyzed here has a well-defined initial momentum (in $\mathcal{B}$) but can be distributed among different bands. At the end of each Bloch period, the amplitude in band α acquires the following phase with respect to the amplitude in band β:

$$\phi_{\alpha\beta} = -\frac{1}{\hbar}\langle\epsilon_\alpha(k) - \epsilon_\beta(k)\rangle T_{\mathrm{B}} = -\frac{2\pi}{F_0}\langle E_\alpha(k) - E_\beta(k)\rangle, \tag{15}$$

where $\langle\ldots\rangle$ denotes the average over $\mathcal{B}$, $E_\gamma(k)$ is the energy of the state with quasimomentum k in band γ in units E_{rec}, and ϵ is the energy without this normalization. We will use the shorthand notation $\langle\Delta E_{\alpha\beta}\rangle = \langle E_\alpha(k) - E_\beta(k)\rangle$ in the following.

We now analyze interband transitions through an effective model. We focus on the experimental parameters of the Pisa setup [15,16] and model transitions from the first band to the second band. In the parameter regime of shallow lattices there is numerical and experimental evidence of a steplike structure of the adiabatic survival probability $P(t)$ [15] in the first band. If the initial state is peaked around $k = 0$ and lies in the first band, the survival probability is characterized by steep drops around times $t = T_{\mathrm{B}}(n + 1/2)$, with n being an integer, and flat plateaus between these times [41]. This view is corroborated by numerical simulations [Fig. 2(a)] and experimental observations [15]. This time evolution is due to the fact that the coupling between the first and the second bands is maximal at the edge of the first Brillouin zone, for $k = \pm\pi/d_L$, and thus significant transitions occur there, with periodicity T_{B}. Figure 2 shows that plateaus are clearly present for $V_0 = 1.5$ [shallow lattice, Fig. 2(a)], but start to wash out for $V_0 = 4.5$ [Fig. 2(b)]. The range of validity of the plateau picture is further discussed in the Appendix and is approximately valid for $V_0 \lesssim 4.5$. In the following analysis we shall focus on this regime.

The approximated dynamics takes into account experimental and numerical evidence and is valid for small values of V_0 and F_0, when the transition times can be considered much smaller than T_{B}. We assume that the evolution inside the first band is adiabatic for all k, except for $k \simeq \pi/d_L$, when a transition toward the state with the same quasimomentum in the second band becomes possible. This transition will be

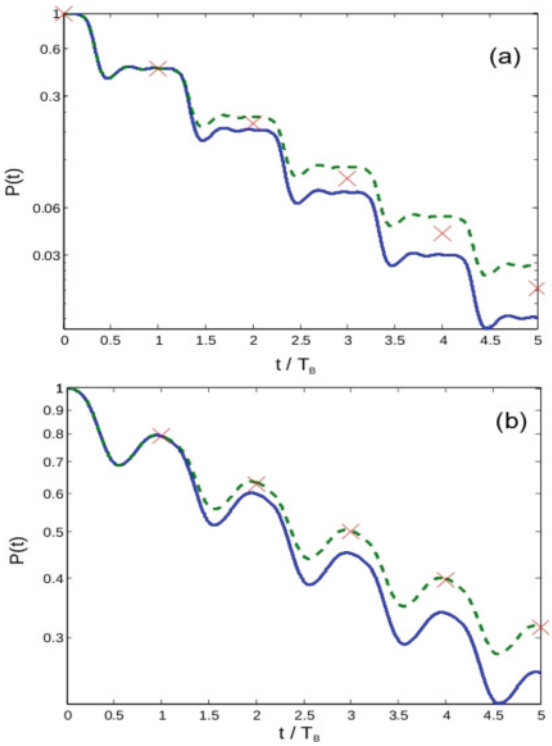

FIG. 2. (Color online) Adiabatic survival probability in the lowest band $P(t)$ vs time, obtained by numerically solving the Schrödinger equation for the atomic evolution under the Hamiltonian of Eq. (11). The initial state has initial quasimomentum $0.2p_{\mathrm{rec}}$ in the Brillouin zone and a negligible quasimomentum width. (a) Potential depth $V_0 = 1.5$ and phase $\phi \simeq 4\pi$ from Eq. (15); (b) $V_0 = 4.5, \phi \simeq 2\pi$. The solid blue line represents the unperturbed time evolution, and the dashed green line represents the time evolution with the phase change discussed in Sec. V B after each Bloch period. The red crosses are an extrapolation of the first time step to the following periods. Plateaus manifest for $V_0 = 1.5$ (a). The validity of this picture is discussed in the text and in the Appendix.

effectively described by the evolution operator of the form

$$\tilde{U} = \begin{pmatrix} s_{12} & -p_{12} \\ p_{12} & s_{12} \end{pmatrix}, \tag{16}$$

with $p_{12} = \sqrt{1 - s_{12}^2}$. The operator $\tilde{U}$ acts on the two-dimensional space spanned by $\{|1\rangle, |2\rangle\}$, where $|1\rangle$ represents the state with $k = \pi/d_L$ in the first band and $|2\rangle$ represents the state with same quasimomentum in the second band.

The transition from the second band to the third band can be schematized as the loss of a fraction $1 - s_{23}^2$ in the population of the second band toward a continuum, occurring at the crossing around $k = 0$. This assumption is justified for small values of V_0 (see discussion above), such that a particle in the third (or higher) band can be considered free.

During each Bloch cycle separating two successive transitions, the relative phase between the second and the first band amplitudes increases by ϕ_{21} from (15), which reads

$$\phi(V_0, F_0) = \phi_{21}(V_0, F_0) = -\frac{2\pi}{F_0}\langle\Delta E(V_0)\rangle, \tag{17}$$

where $\langle\Delta E\rangle = \langle E_2(k) - E_1(k)\rangle$ is the energy difference (in units of E_{rec}) between the second and the first bands, averaged

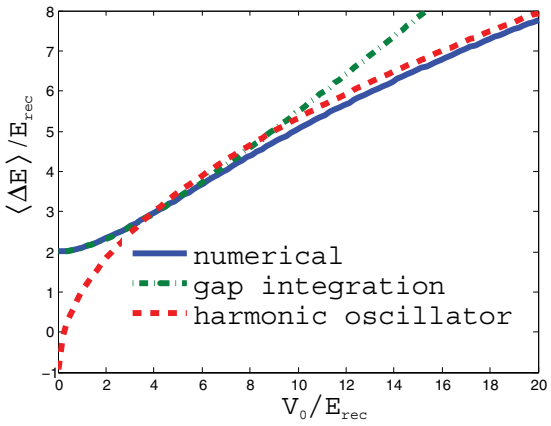

FIG. 3. (Color online) Average band gap $\langle \Delta E \rangle$ vs V_0 (both in units of $E_{\rm rec}$). Comparison between numerical results, analytical results from Eq. (19), and the harmonic oscillator approximation (20). In the small-V regime the band integration yields a good approximation, while for larger V, where the coupling becomes continuous, the harmonic oscillator approximation is more effective.

over $\mathcal{B}$. This energy difference can be exactly computed using Mathieu characteristics $a(\kappa,q)$, which are the eigenvalues of the Mathieu equation [46]

$$\frac{d^2y}{dx^2} + [a - 2q\cos(2x)]\, y = 0, \tag{18}$$

corresponding to the Floquet solutions $y(x) = \exp(i\kappa x)u(x)$. For small V_0, a good estimate is given by

$$\langle \Delta E \rangle \simeq \frac{1}{4}\sqrt{64 + V_0^2} + \frac{V_0^2}{32}\operatorname{arcsinh}\frac{8}{V_0}, \tag{19}$$

which is obtained by integrating the two-level approximation of Eq. (3) for the energy difference of the lowest two bands of Hamiltonian (12) over the Brillouin zone $\mathcal{B}$. For larger V_0, a tight-binding, or harmonic oscillator, approximation yields

$$\langle \Delta E \rangle \simeq \sqrt{4V_0} - 1. \tag{20}$$

The exact result and the two aforementioned approximations are compared in Fig. 3.

The effects of the dynamics in a time $T_{\rm B}$ from one transition to the next one can thus be modeled in the basis $\{|1\rangle, |2\rangle\}$ by an effective nonunitary operator,

$$W = \begin{pmatrix} 1 & 0 \\ 0 & s_{23}e^{i\phi} \end{pmatrix}. \tag{21}$$

By making use of this simplified model, we describe the time evolution in the following way. At $t = 0$ the condensate is in the first band, with quasimomentum close to $k = 0$. As the lattice is accelerated, the quasimomentum increases until it reaches π/d_L at $t = T_{\rm B}/2$, where the operator $\tilde{U}$ comes into play and transfers part of the population to the second band. The evolution from $T_{\rm B}/2$ to $3T_{\rm B}/2$ is summarized by the application of W. Then, the second transition occurs, and part of the population in the second band (decreased by losses toward the third band) can tunnel back to the first band due to the action of $\tilde{U}$ and gives rise to interference effects. The same steps occur in the subsequent transitions.

On a time span $T_{\rm B}$, the dynamics of the system is therefore determined by the successive action of the nonunitary operator,

$$U = \tilde{U}W = \begin{pmatrix} s_{12} & -p_{12}s_{23}e^{i\phi} \\ p_{12} & s_{12}s_{23}e^{i\phi} \end{pmatrix}, \tag{22}$$

in the basis $\{|1\rangle, |2\rangle\}$. The order of the two operations is not relevant since W acts trivially on the "initial state" $|1\rangle$ before the first transition.

Besides the phase ϕ, the operator U depends on two other independent parameters, namely, the survival amplitudes s_{12} and s_{23}. s_{12} represent the survival amplitude in the first band after the *first* transition, which is, in fact, comparable to a LZ process since the second band is initially empty. The survival probability s_{23} is related to a LZ tunneling from the second band to the third band if we assume the third band to be empty before each transition process. A graphical representation of the parameters appearing in Eq. (22) is given in Fig. 1.

Using the LZ critical acceleration for the first and second band gaps [32,33,47,48], analytical expressions for s_{12} and s_{23} as functions of the microscopic parameters can be obtained. At lowest order in V_0, the survival amplitudes read

$$\begin{aligned} s_{12}(V_0,F_0) &= \sqrt{1 - P_{\rm LZ}^{(1,2)}(V_0,F_0)} \\ &= \sqrt{1 - \exp\left(-\frac{\pi^2 V_0^2}{32F_0}\right)}, \end{aligned} \tag{23}$$

$$\begin{aligned} s_{23}(V_0,F_0) &= \sqrt{1 - P_{\rm LZ}^{(2,3)}(V_0,F_0)} \\ &= \sqrt{1 - \exp\left(-\frac{\pi^2 V_0^4}{32 \times 16^2(2F_0)}\right)}, \end{aligned} \tag{24}$$

where $P_{\rm LZ}^{(i,j)}$ is the Landau-Zener transition probability (4) from band i to band j. The evolution on a time scale $T_{\rm B}$, determined by a sequence of U operations, will be analyzed in detail in the following section.

IV. TRANSIENT AND ASYMPTOTIC BEHAVIOR

We now specialize the model outlined in Sec. III to the Pisa experimental setup [15,16]. The state of the system before the first transition is $|1\rangle$. Immediately after the nth transition, occurring at time $t = T_{\rm B}(n + 1/2)$, the state of the system is

$$|\Phi_n\rangle = U^n |1\rangle. \tag{25}$$

The matrix U in Eq. (22) can be diagonalized, yielding eigenvalues (e_1,e_2). By expanding the initial state as

$$|1\rangle = c_1 |\psi_1\rangle + c_2 |\psi_2\rangle, \tag{26}$$

where $|\psi_{1,2}\rangle$ are the normalized *nonorthogonal* eigenvectors of U, the state of the system at time $T_{\rm B}(n + 1/2)$ is

$$|\Phi_n\rangle = c_1 e_1^n |\psi_1\rangle + c_2 e_2^n |\psi_2\rangle. \tag{27}$$

Due to the dissipative term in W, the two eigenvalues are smaller than unity, and one of them, say e_1, is larger in modulus than the other one. Thus, for n sufficiently large, the evolution reaches an asymptotic regime in which the state after the nth transition is determined only by the state after the previous one, with a transition rate depending on the largest eigenvalue. Since the survival probability in the first band can be defined

as $P_n = |\langle 1|\Phi_n\rangle|^2$, in the asymptotic regime one gets

$$P_{n+1} \simeq |e_1|^2 P_n. \tag{28}$$

By defining an asymptotic transition rate

$$\gamma = -\ln(|e_1|^2), \tag{29}$$

it is possible to introduce a function $P_Z(t)$ that coincides with the value of the survival probability at the center of the plateaus at times $t = nT_B$:

$$P_Z(t) = Z \exp(-\gamma t). \tag{30}$$

Observe that Eqs. (28)–(30) are valid in the asymptotic regime. Before reaching it, the ratio between P_n and P_{n-1} in Eq. (28) depends on n through a "time-dependent decay rate" γ_n, as in

$$P_{n+1} = e^{-\gamma_n} P_n, \tag{31}$$

whose asymptotic value is $\gamma = \lim_{n\to\infty} \gamma_n$. See the following discussion and, in particular, Eqs. (36)–(40).

The parameter Z in Eq. (30) is, in general, different from unity, due to the transient regime at the beginning of the evolution. It represents the extrapolation of the asymptotic exponential probability back at $t = 0$.

We now derive an analytical expression for Z. In the asymptotic regime, the system evolution described by Eq. (27) corresponds to an evolution operator applied to an initial unnormalized vector $|\Psi_0\rangle \equiv c_1 |\psi_1\rangle$:

$$|\Phi_n\rangle \simeq c_1 e_1^n |\psi_1\rangle = U^n (c_1 |\psi_1\rangle) = U^n |\Psi_0\rangle. \tag{32}$$

The Z parameter, representing the extrapolation of the asymptotic behavior back to $t = 0$, can be defined as the square modulus of the projection of the fictitious initial vector $|\Psi_0\rangle$ onto the actual initial state $|1\rangle$:

$$Z \equiv |\langle 1|\Psi_0\rangle|^2 = |c_1|^2 |\langle 1|\psi_1\rangle|^2, \tag{33}$$

which corresponds to an extrapolated "survival probability" in the subspace spanned by $|1\rangle$, evaluated at the initial time. Z can be analytically computed as a function of the independent parameters of the model by explicitly diagonalizing U. One obtains

$$Z(s_{12}, s_{23}, \phi) = \frac{\left[\frac{s_{12}}{2}(1 - s_{23}\cos\phi) + \sqrt{\frac{\mathcal{K}(s_{12},s_{23},\phi)}{8}}\right]^2 + s_{23}^2 \sin^2\phi \left[\frac{2 - s_{12}^2(1 + s_{23}\cos\phi)}{\sqrt{2\mathcal{K}(s_{12},s_{23},\phi)}} + \frac{s_{12}}{2}\right]^2}{\frac{\mathcal{K}(s_{12},s_{23},\phi)}{2} + \frac{2 s_{23}^2 \sin^2\phi}{\mathcal{K}(s_{12},s_{23},\phi)}\left[2 - s_{12}^2(1 + s_{23}\cos\phi)\right]^2}, \tag{34}$$

with

$$\mathcal{K}(s_{12}, s_{23}, \phi) = s_{12}^2\left[1 + 2 s_{23}\cos\phi + s_{23}^2\cos(2\phi)\right] - 4 s_{23}\cos\phi + \sqrt{s_{12}^4\left(1 + 2 s_{23}\cos\phi + s_{23}^2\right) - 8 s_{23} s_{12}^2\left(\cos\phi + 2 s_{23} + s_{23}^2\cos\phi\right) + 16 s_{23}^2}. \tag{35}$$

Observe that the above two equations do not depend on the sign of ϕ. In order to gain a qualitative understanding of the dependence of Z (and γ) on the phase difference ϕ acquired during a Bloch cycle, let us compare the first and second transitions. Let $P_0 = 1$ be the initial value of the survival probability in the first band. After the first transition, the survival probability becomes

$$P_1 = s_{12}^2 P_0 \equiv e^{-\gamma_0} P_0. \tag{36}$$

At the second transition, the discrepancy with the LZ prediction becomes manifest. Since, in the parameter regime of small V_0 we are considering, the ratio s_{23}/s_{12} is very small [see Eqs. (23) and (24)], we can apply a first-order approximation, yielding

$$P_2 \simeq \left(s_{12}^2 - 2 s_{23} p_{12}^2 \cos\phi\right) P_1 \equiv e^{-\gamma_1} P_1. \tag{37}$$

Thus, if the phase ϕ, introduced in Eq. (17), is $\phi = 2\pi j$, with $j \in \mathbb{Z}$, the second transition is enhanced with respect to the first one. In this case, a local maximum in the transition rate as a function of F_0 is expected. On the contrary, if $\phi = (2j + 1)\pi$, the second transition is less pronounced than the first one.

A backward extrapolation of the second step gives a rough estimate of the Z parameter, which we call Z_1:

$$Z \simeq Z_1 = e^{\gamma_1 - \gamma_0} \simeq 1 + 2 s_{23}\left(\frac{p_{12}}{s_{12}}\right)^2 \cos\phi. \tag{38}$$

Even if Eq. (38) represents a rather crude approximation, it brings to light the correspondence between resonances in the asymptotic transition rates and resonances in the Z parameter. Quantities like (38) are very useful in an experimental context, where only the first few steps in the Bloch cycles are accessible. If the survival amplitude can be measured up to the Nth transition, the Z parameter can be approximated by

$$Z \simeq Z_N = e^{N\gamma_N - \sum_{n=0}^{N-1}\gamma_n}. \tag{39}$$

At the same time,

$$\gamma \simeq \gamma_N. \tag{40}$$

The convergence to the real value of Z is typically very fast, and the first few cycles are already sufficient to obtain an excellent approximation.

The estimates of Eqs. (17)–(23), together with Eq. (34), enable one to obtain an analytical expression $Z(V_0, F_0)$, yielding the value of Z as a function of the microscopic parameters.

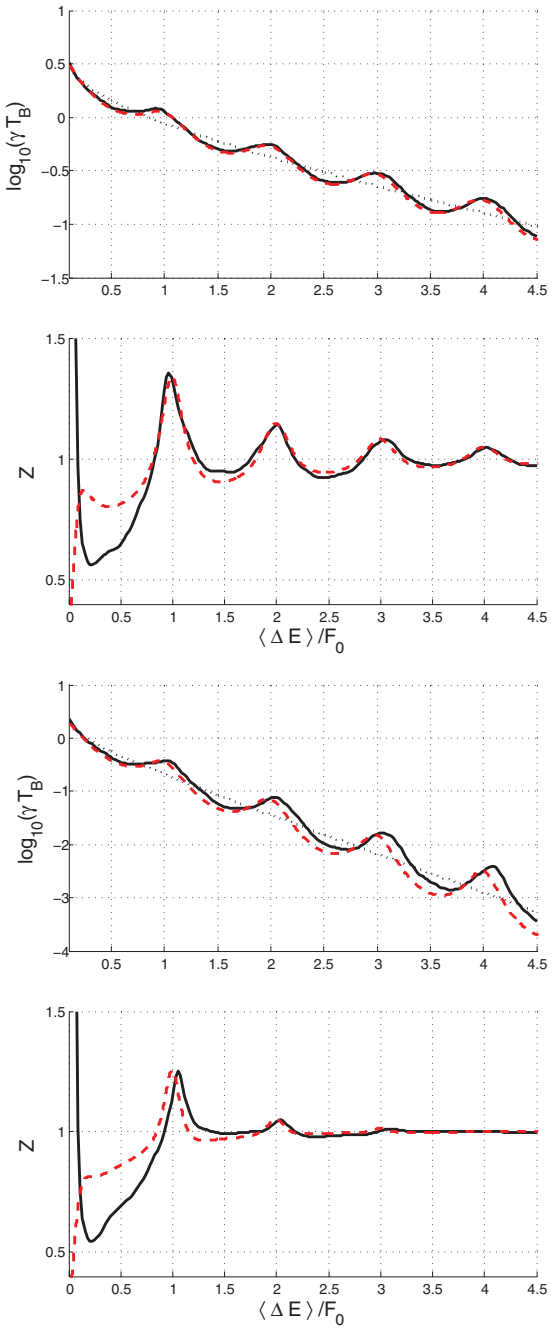

FIG. 4. (Color online) Decay rate γ and wave-function renormalization Z vs $\langle \Delta E \rangle / F_0 = \phi / 2\pi$. Comparison among analytical results, obtained by exact diagonalization of the reduced evolution operator U in Eq. (22) (red dashed lines), numerical simulations based on Eq. (11) (solid lines), and Landau-Zener prediction (dotted lines for γ). $V_0 = 2$ in the first two panels, and $V_0 = 4$ in the bottom two panels.

Figure 4 shows a comparison of the numerical calculation and the estimates for γ and Z with our analytical model. It is clear that the model yields a better approximation for smaller V_0. For $V_0 \gtrsim 4.5$ the peaks of Z are overestimated, and the picture of successive tunneling events with an intermediate phase accumulation becomes less valid. In the regime of small V_0, the analytical model is very efficient, as long as F_0 is not too large and the LZ tunneling rates do not have to be adjusted due to the finite initial time of the evolution [37].

V. EXPERIMENTAL CONFIGURATIONS

This section contains a discussion of the experiments performed up to now and suggestions for future measurements aimed at controlling the decay by a manipulation of the phase of the temporally evolved atomic wave packet. The relations of Sec. IV can be tested experimentally as follows.

A. Measurement of $P(t)$

An experimental check of the theory at the basis of the wave-function renormalization Z is obtained by measuring the survival probability $P(t)$ for a time up to five Bloch periods for different parameter values, as in Fig. 2, and then introducing a fit with the exponential law of Eq. (30) for the survival probability at times $t = nT_B$. The Z and γ parameters are determined by such a fit. The results of this approach are discussed in the following for the case of a narrow atomic momentum distribution, as in the RET experiments at Pisa with a Bose-Einstein condensate [12,13,15,16], and for the case of a broad atomic momentum distribution, as for the experiment performed at Austin [26,27].

1. Pisa RET experiment

The time dependence of the adiabatic survival probability was measured by freezing the tunneling process through projective quantum measurements on the states of the adiabatic Hamiltonian [15]. Experimental results of $P(t)$ for different values of the lattice depth and the applied force are shown in Fig. 5. The solid and dashed lines are a numerical simulation of our experimental protocol and an exponential decay fit for our system's parameters, respectively. The vertical intercept of the exponential decay at $t = 0$ gives the value of Z, and the exponential decay rate gives the value of γ.

The resonant tunneling appears as a strong variation for the exponential decay rate of γ as a function of ϕ, as measured in the experiments [12,13]. This variation matches the numerical predictions of Fig. 4.

Measured values of the Z parameter vs the ϕ parameter are plotted in Fig. 6(a). The error bars on the Z values are determined by the exponential fits, as in Fig. 5. Notice that Z values both larger and smaller than 1 are measured. The error of the phase ϕ is linked to the experimental accuracy of the V_0 and F_0 parameters (V_0 carries an error of around 10%). The experimental results are compared to theoretical predictions for the numerical solutions of the time-dependent adiabatic survival probability. The peaks in the plot are determined by RET resonances. The simulation of Fig. 4 evidences that the dependence of Z on ϕ matches the dependence of γ. The position of the largest peak corresponds to the main resonance [12,13] $\Delta i = 1$, and the positions of the smaller peaks are in agreement with those of higher-order resonances. The agreement between the theoretical and experimental determinations of Z is very good, taking into account the difficulties of a precise determination of the lattice depth V_0. It should be noticed *a posteriori* that the experimental results are more easily produced in the case $Z < 1$.

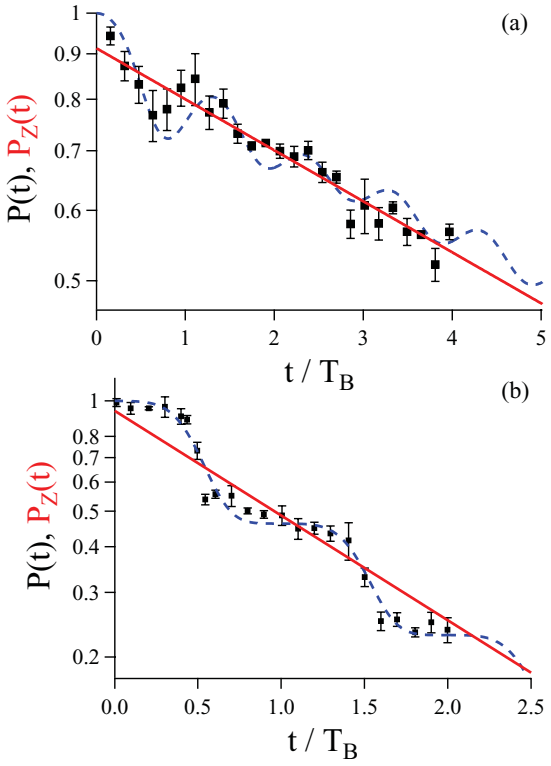

FIG. 5. (Color online) $P(t)$: experimental results (squares) and numerical solution of the Schrödinger equation describing the atomic cloud within the accelerated optical lattice (blue dashed line). The red solid lines are exponential fits to the experimental data based on $P_Z(t)$ from Eq. (30), whose crossing with the y axis yields the value of Z. In (a) $V_0 = 5.8E_{\rm rec}$, $F_0 = 5$, and in (b) $V_0 = 1E_{\rm rec}$, $F_0 = 0.383$. Both cases yield $Z < 1$. The slope of the exponential decay gives the decay rate γ.

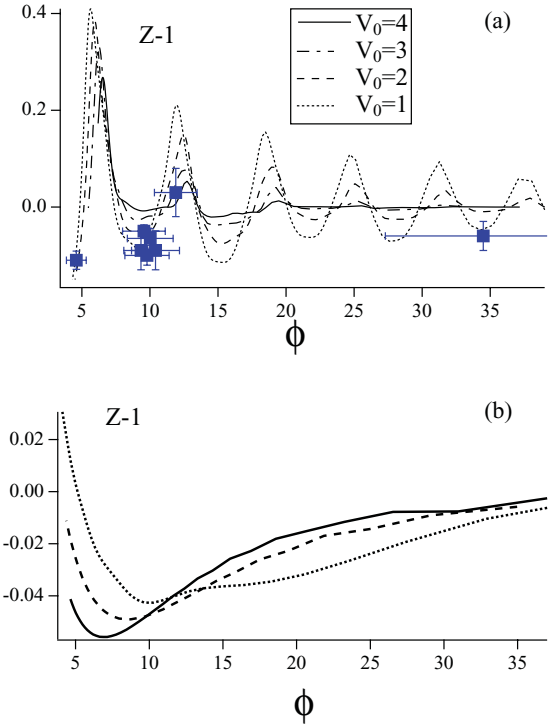

FIG. 6. (Color online) (a) Scaling plot of $Z - 1$ vs ϕ of Eq. (17), derived from RET experimental results (squares) using a narrow atomic quasimomentum distribution. The experimental point at $\phi = 4.8$ is obtained from the data of Fig. 5(a), and the point at $\phi = 34$ is obtained from the data of Fig. 5(b). Lines are the theoretical predictions for $V_0 = 1,2,3,4$ (dotted, dashed, dot-dashed, and solid lines, respectively). The RET coupling yields the oscillating behavior of Z vs ϕ, with the oscillation amplitudes increasing at lower V_0 for a fixed ϕ. (b) Theoretical prediction for $Z - 1$ in an Austin-type experiment, with a broad atomic quasimomentum distribution, at $V_0 = 3,3.5$, and 4 (solid, dashed, and dotted lines, respectively).

2. *Austin experiment on nonexponential decay*

The very broad atomic distribution of the experiment performed by Raizen's group in Texas [26,27], occupying several Brillouin zones, leads to a different temporal evolution of the survival probability. In particular, the deeper lattice potentials used in these works imply a different behavior of the Z function. The survival probability was numerically evaluated on the basis of the theoretical treatment reported in Niu and Raizen [49] and Wilkinson *et al.* [26]. For the case of Rb atoms and parameters very close to those experimentally investigated in Pisa, Fig. 6(b) reports the Z function versus the parameter ϕ at a fixed value of the lattice depth. It may be noticed that the values of $|Z - 1|$ are smaller than those measured in the case of a narrow atomic quasimomentum distribution. The Z dependence on F_0 is very smooth, without the oscillations of Fig. 6(a). The Niu-Raizen theory [26,49] includes only the two lowest-energy bands and does not take into account tunneling phenomena such as RET or higher-excited-energy bands. The Niu-Raizen model is thus essentially a two-state model for Landau-Zener coupling, neglecting resonant tunneling effects, and averaged over all quasimomenta in the entire Brillouin zone. Such a model is better suited for large values of V_0, when the energy bands become flat.

B. Phase control

To further verify that the phase ϕ is, indeed, the important quantity determining the temporal evolution of the atomic wave function, it could be interesting to perform a LZ experiment for which the atomic acceleration is stopped after each Bloch period for a time $t_{\rm halt} = \pi/\Delta E$, with ΔE being the energy difference between the two bands, in order to reverse the phase of the wave function's evolution. Differences in the predicted time dependence of $P(t)$ with and without this phase reversal are reported in Fig. 2. Even if the experimental error introduced by the phase imprinting could be too large to derive Z precisely in this regime, the observation of a modified decay rate in the presence of a phase reversal would represent a direct proof that ϕ is responsible for the resonances in the decay rate.

The survival probability obtained in an experiment where after each period one halts or does not halt with equal probability represents another tool for modifying and testing the interference in successive Landau-Zener processes. The change of the decay rate by this randomization is equivalent to the change that would be obtained via *bona fide* quantum measurements, as in the standard formulation of the Zeno

effect, which was experimentally observed in Ref. [27]. It can be demonstrated that the same atomic evolution is obtained by performing nondestructive survival probability measurements after each Bloch period, with the quantum Zeno effect being achieved in the limit of very frequent measurements carried out within a Bloch period.

C. Emptying the second band

A similar interesting experimental configuration is realized by totally eliminating the second band's occupation after each Bloch period. This could be produced as in the measurement protocol used in Ref. [15] by decreasing the acceleration after each tunneling event from the ground band down to a small value such that the population in the second band tunnels to the continuum and is no longer confined by the optical lattice. At the same time the population in the lower band does not tunnel to the second one and is ready to be accelerated once again with the original large value. In this kind of setup all Landau-Zener steps in the survival probability as a function of time would have the same height on a logarithmic scale, determined by s_{12} only. The phase ϕ would then be totally irrelevant to the atomic evolution.

D. Links with quantum field theory

Finally, from a theoretical perspective, it would be of great interest to explore the links with wave-function-renormalization effects in quantum field theory. In that context, the quantity Z arises from an analysis of the propagator (enforcing probability conservation in the Källén-Lehmann representation [50,51]) and differs from unity at second order in the coupling constant. Z is smaller than unity for stable states but is unconstrained and can become >1 for an unstable state. There have been a few attempts [52–58] to analyze the quantum Zeno effect in the decay of elementary particles, but no experiment has been performed so far. It would be interesting to try and mimic these effects by making use of RET in BECs. This would take us into the realm of quantum simulations.

VI. CONCLUSION AND OUTLOOK

In the pioneering work by Raizen *et al.* [26,27] the focus was on the deviations from exponential decay and the occurrence of the quantum Zeno effect and its inverse [29,30] due to repeated measurements. In the present article we endeavored to go further and studied Landau-Zener transitions [32,33] under very different physical conditions, both in terms of initial state and parameters. This enabled us to use these effects as a bench test for the study of wave-function-renormalization effects in quantum mechanics. We have seen that by scrutinizing the features of the survival probability of the wave function that collectively describes an ultracold atomic cloud, one can consistently define Z and extract crucial information on its behavior. It is remarkable that Z can be directly measured and that its deviation from unity yields directly measurable consequences on the experimental observables. In addition, as the experimental parameters are varied, Z takes values that can be smaller or larger than unity. If $Z < 1$, the decay can be slowed down (quantum Zeno effect) or enhanced (anti- or inverse-Zeno effect), but if $Z > 1$, only the quantum Zeno effect is possible [21].

Our analysis of the atomic evolution in terms of successive free evolutions and tunneling processes, with interference in the population occupations, points out that Landau-Zener transitions and Stückelberg oscillations [34] are two facets (one could say particular cases) of the very complex problem of the atomic evolution within the periodic potential produced by the optical lattice, in analogy to a previous analysis by Kling *et al.* [59].

For the shallow lattice regime, we have established a relationship between γ, Z, and $\phi = 2\pi\langle\Delta E(V_0)\rangle/F_0$. We have demonstrated that the Zeno regime and resonantly enhanced tunneling are both controlled by the same parameter ϕ in an ultracold atomic cloud. The resonances in Z can be explained by a decay following the Landau-Zener probability in the first Bloch period and resonantly enhanced decay in the following periods. In contrast, the Niu-Raizen description [49] applied to describe the nonexponential decay of cold atoms in an optical lattice approximates the tunneling rate from the second band to the third band by one complete decay. In the large V_0 parameter regime the RET resonances are not important and do not affect the quantum Zeno effect.

A future experiment could involve a BEC atomic cloud in the presence of atomic interactions [12,13,39–45,60].

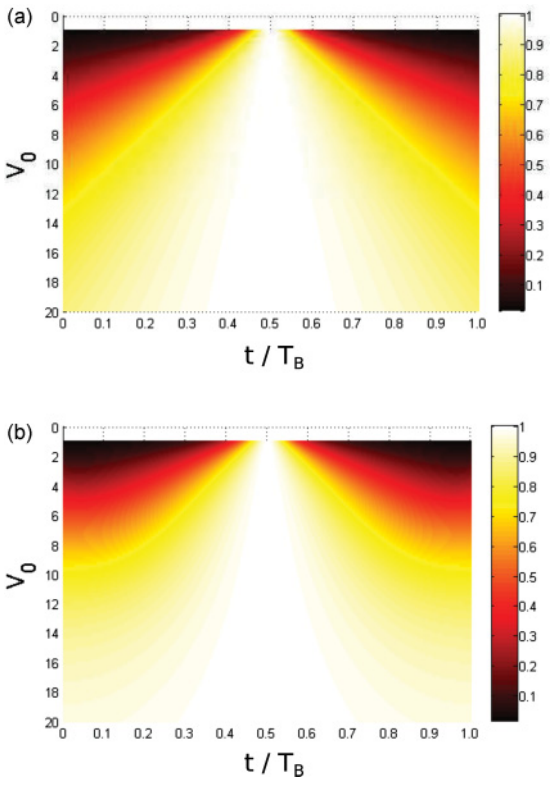

FIG. 7. (Color online) Adiabatic coupling strength $c(t)$, defined in Eq. (A4) and normalized to maximal coupling, plotted vs time and optical lattice depth. Comparison between (a) the Lorentzian ansatz and (b) numerical results based on Eq. (11). The assumption of short tunneling events at the avoided crossings is valid for $V_0 \lesssim 4.5$ in units of $E_{\rm rec}$ (shallow lattice).

As verified experimentally [39], in this case the tunneling probabilities are not symmetric ($s_{ij} \neq s_{ji}$), and the effect of the RET resonances could be enhanced or suppressed with attractive or repulsive interactions.

ACKNOWLEDGMENTS

E.A., D.C., R.M., and O.M. acknowledge support from the E.U. through Grant No. 225187-NAMEQUAM and from MIUR through PRIN2009. P.F. and G.F. acknowledge support by the project IDEA of Università di Bari. N.L. and S.W. are very grateful for the cordial hospitality in Pisa and for support by the DFG (FOR760, WI 3426/3-1), the Helmholtz Alliance Program EMMI (HA-216), and the HGSFP (GSC 129/1).

APPENDIX: CHECK ON THE INTERRUPTED ATOMIC EVOLUTION

The dynamics of interband tunneling is discussed in Sec. III and hinges on the assumption of a free phase evolution over the Brillouin zone, interrupted by a very short tunneling event at the avoided crossing, at well-defined times $t = T_B(n + 1/2)$ with $n \in \mathbb{N}$, as in Figs. 2(a) and 5(b). To check the validity of this assumption we use the Hamiltonian H_a, which describes the time evolution in the adiabatic (energy) basis. H_a can be obtained by expanding the state $|\psi(t)\rangle$ of the system in the time-dependent energy basis,

$$|\psi(t)\rangle = \sum_n a_n(t)\,|n(t)\rangle, \tag{A1}$$

and applying the Schrödinger equation $i\,\partial_t\,|\psi\rangle = H\,|\psi\rangle$ with the Hamiltonian of Eq. (12) to obtain

$$i \sum_n (\dot{a}_n\,|n\rangle + a_n\,\partial_t\,|n\rangle) = \sum_n a_n E_n\,|n\rangle. \tag{A2}$$

Taking the inner product with $\langle m|$ and using $\langle m|n\rangle = \delta_{mn}$, we get

$$\dot{a}_m = -i\,E_m a_m - \sum_n \langle m|\,\partial_t\,|n\rangle\,a_n, \tag{A3}$$

and we see that the off-diagonal term coupling the lowest two energy states is given by

$$c(t) := \langle 1|\,\partial_t\,|2\rangle. \tag{A4}$$

In the ideal Landau-Zener model of Eq. (2) and Ref. [31] this yields for $c(t)$ a Lorentzian function of time in a narrow time interval centered around the $T_B/2$ transition time. The Lorentzian is displayed in Fig. 7(a) for different values of the potential depth V_0. Figure 7(b) shows the numerical result for $c(t)$ in our system. The model discussed in Sec. III ceases to be valid when c is large, at the border of the Brillouin zone. A comparison of the two plots in Fig. 7 clarifies that the approximations used in our analysis break down for $V_0 \gtrsim 4.5$.

[1] D. Bohm, in *Quantum Theory* (Dover, New York, 1989), p. 286.
[2] L. L. Chang, E. E. Mendez, and C. Tejedor, eds., *Resonant Tunneling in Semiconductors* (Plenum, New York, 1991).
[3] L. L. Chang, L. Esaki, and R. Tsu, Appl. Phys. Lett. **24**, 593 (1974).
[4] L. Esaki, IEEE J. Quantum Electron. **22**, 1611 (1986).
[5] S. Glutsch, Phys. Rev. B **69**, 235317 (2004).
[6] M. Wagner and H. Mizuta, Phys. Rev. B **48**, 14393 (1993).
[7] K. Leo, *High-Field Transport in Semiconductor Superlattices* (Springer, Berlin, 2003).
[8] G. Grynberg and C. Robilliard, Phys. Rep. **355**, 335 (2001).
[9] O. Morsch and M. Oberthaler, Rev. Mod. Phys. **78**, 179 (2006).
[10] I. Bloch, Nat. Phys. **1**, 1 (2005).
[11] I. Bloch, J. Dalibard, and W. Zwerger, Rev. Mod. Phys. **80**, 885 (2008).
[12] C. Sias, A. Zenesini, H. Lignier, S. Wimberger, D. Ciampini, O. Morsch, and E. Arimondo, Phys. Rev. Lett. **98**, 120403 (2007).
[13] A. Zenesini, C. Sias, H. Lignier, Y. Singh, D. Ciampini, O. Morsch, R. Mannella, E. Arimondo, A. Tomadin, and S. Wimberger, New J. Phys. **10**, 053038 (2008).
[14] M. Glück, A. R. Kolovsky, and H. J. Korsch, Phys. Rep. **366**, 103 (2002).
[15] A. Zenesini, H. Lignier, G. Tayebirad, J. Radogostowicz, D. Ciampini, R. Mannella, S. Wimberger, O. Morsch, and E. Arimondo, Phys. Rev. Lett. **103**, 090403 (2009).
[16] G. Tayebirad, A. Zenesini, D. Ciampini, R. Mannella, O. Morsch, E. Arimondo, N. Lörch, and S. Wimberger, Phys. Rev. A **82**, 013633 (2010).
[17] A. Messiah, *Quantum Mechanics*, Sec. XXI-13 (Dover, New York, 1999).
[18] C. Cohen-Tannoudji, J. Dupont-Roc, and G. Grynberg, *Atom-Photon Interactions: Basic Processes and Applications* (Wiley-VHC, New York & Berlin, 1998).
[19] S. Weinberg, *The Quantum Theory of Fields*, *Foundations*, Vol. 1 (Cambridge University Press, Cambridge, 1995).
[20] M. Peskin and D. Schoeder, *An Introduction to Quantum Field Theory* (Addision Wesley, Reading, 1995).
[21] P. Facchi, H. Nakazato, and S. Pascazio, Phys. Rev. Lett. **86**, 2699 (2001).
[22] H. Nakazato, M. Namiki, and S. Pascazio, Int. J. Mod. Phys. B **10**, 247 (1996).
[23] B. Misra and E. C. G. Sudarshan, J. Math. Phys. **18**, 756 (1977).
[24] P. Facchi and S. Pascazio, in *Fundamental Aspects of Quantum Physics: Proceedings of the Japan-Italy Joint Workshop on Quantum Open Systems, Quantum Chaos and Quantum Measurement: Waseda University, Tokyo, Japan, 27–29 September 2001* (World Scientific, Singapore, 2003), p. 222.
[25] L. A. Khalfin, Dokl. Acad. Nauk USSR **115**, 277 (1957) [Sov. Phys. Dokl. **2**, 340 (1957)]; Zh. Eksp. Teor. Fiz. **33**, 1371 (1958) [Sov. Phys. JETP **6**, 1053 (1958)].
[26] S. Wilkinson, C. Bharucha, M. Fischer, K. Madison, Q. Niu, B. Sundaram, and M. G. Raizen, Nature (London) **387**, 575 (1997).
[27] M. C. Fischer, B. Gutiérrez-Medina, and M. G. Raizen, Phys. Rev. Lett. **87**, 040402 (2001).
[28] A. M. Lane, Phys. Lett. A **99**, 359 (1983).

[29] S. Pascazio and P. Facchi, Acta Phys. Slovaca **49**, 557 (1999); P. Facchi and S. Pascazio, Phys. Rev. A **62**, 023804 (2000).
[30] A. G. Kofman and G. Kurizki, Acta Phys. Slovaca **49**, 541 (1999); Nature (London) **405**, 546 (2000).
[31] N. V. Vitanov, Phys. Rev. A **59**, 988 (1999).
[32] L. Landau, Phys. Z. Sowjetunion **2**, 46 (1932).
[33] C. Zener, Proc. R. Soc. London, Ser. A **137**, 696 (1932).
[34] E. C. G. Stückelberg, Helv. Phys. Acta **5**, 369 (1932).
[35] E. Majorana, Nuovo Cimento **9**, 43 (1932).
[36] H. Jones and C. Zener, Proc. R. Soc. **144**, 101 (1934).
[37] M. Holthaus, J. Opt. B **2**, 589 (2000).
[38] L. Pitaevskii and S. Stringari, *Bose-Einstein Condensation* (Clarendon, Oxford, 2003).
[39] M. Jona-Lasinio, O. Morsch, M. Cristiani, N. Malossi, J. H. Müller, E. Courtade, M. Anderlini, and E. Arimondo, Phys. Rev. Lett. **91**, 230406 (2003).
[40] E. Arimondo and S. Wimberger, in *Dynamical Tunneling*, edited by S. Keshavamurthy and P. Schlagheck (CRC Press, Boca Raton, FL, 2011).
[41] S. Wimberger, R. Mannella, O. Morsch, E. Arimondo, A. R. Kolovsky, and A. Buchleitner, Phys. Rev. A **72**, 063610 (2005).
[42] S. Wimberger, D. Ciampini, O. Morsch, R. Mannella, and E. Arimondo, J. Phys. Conf. Ser. **67**, 012060 (2007).
[43] D. Witthaut, E. M. Graefe, S. Wimberger, and H.-J. Korsch, Phys. Rev. A **75**, 013617 (2007); K. Rapedius, C. Elsen, D. Witthaut, S. Wimberger, and H.-J. Korsch, *ibid.* **82**, 063601 (2010).
[44] S. Wimberger, P. Schlagheck, and R. Mannella, J. Phys. B. **39**, 729 (2006); P. Schlagheck and S. Wimberger, Appl. Phys. B **86**, 385 (2007).
[45] G. Tayebirad, R. Mannella, and S. Wimberger, Appl. Phys. B **102**, 489 (2011).
[46] E. G. C. Poole, *Introduction to the Theory of Differential Equations* (Clarendon, Oxford, 1936).
[47] D. Iliescu, S. Fishman, and E. Ben-Jacob, Phys. Rev. B **46**, 14675 (1992).
[48] Q. Niu, X. G. Zhao, G. A. Georgakis, and M. G. Raizen, Phys. Rev. Lett. **76**, 4504 (1996).
[49] Q. Niu and M. G. Raizen, Phys. Rev. Lett. **80**, 3491 (1998).
[50] G. Källén, Helv. Phys. Acta **25**, 417 (1952).
[51] H. Lehmann, Nuovo Cimento **11**, 342 (1954).
[52] I. Joichi, Sh. Matsumoto, and M. Yoshimura, Phys. Rev. D **58**, 043507 (1998); **58**, 045004 (1998).
[53] P. Facchi and S. Pascazio, Phys. Lett. A **241**, 139 (1998); Phys. A **271**, 133 (1999).
[54] P. Facchi, S. Pascazio, and A. Scardicchio, Phys. Rev. Lett. **83**, 61 (1999).
[55] C. Bernardini, L. Maiani, and M. Testa, Phys. Rev. Lett. **71**, 2687 (1993).
[56] R. F. Alvarez-Estrada and J. L. Sánchez-Gómez, Phys. Lett. A **253**, 252 (1999).
[57] F. Giacosa and G. Pagliara, Mod. Phys. Lett. A **26**, 2247 (2011).
[58] G. Pagliara and F. Giacosa, Acta Phys. Pol. B. Proc. Suppl. **4**, 753 (2011).
[59] S. Kling, T. Salger, C. Grossert, and M. Weitz, Phys. Rev. Lett. **105**, 215301 (2010).
[60] D. I. Choi and Q. Niu, Phys. Rev. Lett. **82**, 2022 (1999); O. Zobay and B. M. Garraway, Phys. Rev. A **61**, 033603 (2000).